

THE LORENTZ INTEGRAL TRANSFORM (LIT) METHOD

Winfried Leidemann

Dipartimento di Fisica, Università di Trento

and Istituto Nazionale di Fisica Nucleare,

Gruppo Collegato di Trento

Via Sommarive 14,

I-38100 Trento, Italy

leideman@science.unitn.it

(Dated: November 1, 2018)

Abstract

The LIT approach is reviewed both for inclusive and exclusive reactions. It is shown that the method reduces a continuum state problem to a bound-state-like problem, which then can be solved with typical bound-state techniques. The LIT approach opens up the possibility to perform *ab initio* calculations of reactions also for those particle systems which presently are out of reach in conventional approaches with explicit calculations of many-body continuum wave functions. Various LIT applications are discussed ranging from particle systems with two nucleons up to particle systems with seven nucleons.

I. INTRODUCTION

Ab initio calculations are a central element of few-body physics. The only input in such calculations is a well defined Hamiltonian. In nonrelativistic nuclear physics one then solves the Schrödinger – or equivalent – equations without introducing any approximation. In order to calculate cross sections for reactions, where final or initial states are scattering states in the continuum, one is faced with the problem of an *ab initio* calculation of such continuum states. It is well known that already the calculation of a three-body continuum wave function is quite difficult and that today a complete four-body calculation, with all possible break-up channels open, is out of reach. However, the problem of a many-body continuum state calculation can be circumvented if one uses the Lorentz integral transform (LIT) method [1]. In fact the LIT approach allows the *ab initio* calculation of reaction cross sections, where a many-body continuum is involved, without requiring the knowledge of the generally complicated many-body continuum wave function. The scattering problem is reduced to a calculation of a localized function with an asymptotic boundary condition similar to a bound-state wave function. Such an approach was already proposed by Efros in 1985, but with the Stieltjes instead of the Lorentz integral transform [2]. However, it has been found that the application of the Stieltjes transform is problematic since it leads to serious inversion problems [3].

The LIT method has been applied to various electroweak cross sections in the nuclear mass range from $A=3$ to $A=7$. Among the applications are the first realistic *ab initio* calculations of the nuclear three- and four-body total photoabsorption cross sections [4, 5], as well as of the inelastic neutral current neutrino scattering off ${}^4\text{He}$ [6]. In addition first *ab initio* calculations have been performed for the total photoabsorption cross sections of ${}^4\text{He}$ and ${}^{6,7}\text{Li}$ with semirealistic forces [7, 8, 9]. Other applications were carried out for the inelastic inclusive electron scattering cross section (see *e.g.* [10, 11, 12]). Besides inclusive electroweak reactions also LIT calculations of exclusive reactions have been performed, namely for ${}^4\text{He}(\gamma, n){}^3\text{He}$ and ${}^4\text{He}(\gamma, p){}^3\text{H}$ [13], ${}^4\text{He}(e, e'p){}^3\text{H}$ [14], and ${}^4\text{He}(e, e'd)d$ [15]. Further applications and a detailed description of the LIT method are presented in a recent review article [16].

The paper is organized as follows. In section II the general form of inclusive and exclusive cross sections of a particle system induced by an external probe is outlined. Sections III and

IV describe the LIT approach for inclusive and exclusive response functions, respectively. In section V various LIT applications are discussed.

II. STRUCTURE OF ELECTROWEAK CROSS SECTIONS

Perturbation-induced reactions can be divided in inclusive and exclusive processes. In the former case the final state of the particle system is not observed. In the latter case the final state is at least partially observed, like *e.g.* in an $(e, e'p)$ reaction, where besides the scattered electron also an outgoing proton with energy E_p and scattering angle $\Omega_p = (\theta_p, \Phi_p)$ is detected.

Inclusive cross sections of perturbation-induced reactions have the following general form (see *e.g.* [17])

$$\frac{d^2\sigma}{d\omega d\Omega_{ext}} = \alpha_{ext} \sum_{i=1}^M f_i(\omega, q, \theta_{ext}) R_i(\omega, q), \quad (1)$$

where ω and q are energy and momentum transfer of the external probe to the particle system, $\Omega_{ext} = (\theta_{ext}, \phi_{ext})$ denotes the scattering angle of the external probe, α_{ext} is a constant characteristic for the external probe, and f_i are kinematic functions. The functions R_i describe the various responses of the particle system to the external probe and thus contain information about the dynamics of the particle system. They are defined as follows

$$R_i(\omega, q) = \int_{\mathcal{F}} |\langle f | \Theta_i | 0 \rangle|^2 \delta(\omega - (E_f - E_0)). \quad (2)$$

Here E_0 and $|0\rangle$ are ground state energy and wave function of the particle system under consideration, E_f and $|f\rangle$ denote final state energy and wave function of the final particle system, and Θ_i is the operator inducing the response function R_i .

As an example for an exclusive cross section we consider the $(e, e'p)$ case, here one has

$$\frac{d^3\sigma}{d\omega d\Omega_e d\Omega_p} = \alpha_{ext} \sum_{i=1}^N f_i(\omega, q, \theta_e) g_i(\phi_p) r_i(\omega, q, \theta_p, E_p), \quad (3)$$

where the ϕ_p dependence of the cross sections is described by the known functions $g_i(\phi_p)$. Exclusive response functions r_i do not have such a simple form as the inclusive functions R_i . For their definition we refer to [17], here we only mention that transition matrix elements from the ground state $|0\alpha\rangle$ to a specific final state $|f\beta\rangle$,

$$T_{0f,i}^{\alpha\beta} = \langle f\beta | \Theta_i | 0\alpha \rangle, \quad (4)$$

are their essential ingredients, where α and β stand for additional quantum numbers of initial and final state wave functions.

The following relation between the inclusive R_i of (1) and the exclusive r_i of (3) holds:

$$R_i(\omega, q) = \int d\Omega_p dE_p g_i(\phi_p) r_i(\omega, q, \theta_p, E_p). \quad (5)$$

Note that the number of exclusive response functions is generally greater than the number of inclusive ones ($N > M$), since the integration over the azimuthal angle of the outgoing particle can yield zero, *i.e.* the integration over ϕ_p in the $(e, e'p)$ example above.

With additional polarization degrees of freedom for beam and/or target and/or outgoing particles many more additional inclusive and exclusive response functions can be defined (see *e.g.* the deuteron case in [18]).

III. CALCULATION OF INCLUSIVE RESPONSES WITH THE LIT METHOD

As already mentioned, with the LIT method one avoids the explicit calculation of scattering wave functions. Instead, for the calculation of R_i of (2) one proceeds in the following way. One first calculates the ground state wave function $|0\rangle$ of the particle system in question. Then one solves the equation

$$(H - E_0 - \sigma_R - i\sigma_I)|\tilde{\Psi}_i\rangle = \Theta_i|0\rangle, \quad (6)$$

where H is the Hamiltonian of the particle system and $\sigma_{R/I}$ are parameters, whose meaning is explained below. Since the eigenvalues of H have to be real the homogeneous version of (6) has only the trivial solution $\tilde{\Psi}_i = 0$ and thus (6) has a unique solution. In addition, due to the asymptotically vanishing ground state wave function $|0\rangle$ also the right-hand-side of (6) vanishes asymptotically. Therefore, and because of the complex energy $E_0 - \sigma_R - i\sigma_I$, $\tilde{\Psi}_i$ has a similar asymptotic boundary condition as a bound state. It means that $\tilde{\Psi}_i$ is a so-called localized function, *i.e.* square-integrable with a norm $\langle\tilde{\Psi}_i|\tilde{\Psi}_i\rangle$. This has very important consequences: even if the aim is a calculation of a reaction cross section in the continuum, one is not confronted with a scattering state problem any more, in fact one needs to apply only bound-state techniques for the solution of (6).

The key point of the LIT method consists in the fact that the Lorentz integral transform

L_i of the response function R_i ,

$$L_i(\sigma_R, \sigma_I, q) = \int R_i(\omega, q) \mathcal{L}(\omega, \sigma_R, \sigma_I) d\omega \quad (7)$$

is related to the norm $\langle \tilde{\Psi}_i | \tilde{\Psi}_i \rangle$, which can be obtained from the solution of (6). In fact one has

$$L_i(\sigma_R, \sigma_I, q) = \langle \tilde{\Psi}_i(\sigma_R, \sigma_I, q) | \tilde{\Psi}_i(\sigma_R, \sigma_I, q) \rangle \quad (8)$$

(q dependence of L_i and $\tilde{\Psi}_i$ will be dropped in the following). In (7) \mathcal{L} is a Lorentzian centered at σ_R with a width $\Gamma = 2\sigma_I$:

$$\mathcal{L}(\omega, \sigma_R, \sigma_I) = \frac{1}{(\omega - \sigma_R)^2 + \sigma_I^2}. \quad (9)$$

Now also the meaning of the parameters $\sigma_{R/I}$ becomes evident: σ_I represents a kind of energy resolution, while with σ_R a given energy range can be scanned.

With the above equations the principle idea of the LIT method can be explained: one solves the LIT equation (6) for many values of σ_R and a fixed σ_I , calculates $L_i(\sigma_R, \sigma_I = \text{const})$, and then one inverts the transform in order to determine $R_i(\omega, q)$.

Before coming to the inversion we first want to derive the relation (8). Starting from the definition of L_i in (7) one has

$$L_i(\sigma_R, \sigma_I) = \int d\omega \frac{R_i(\omega, q)}{(\omega - \sigma_R)^2 + \sigma_I^2} = \int d\omega \frac{R_i(\omega, q)}{(\omega - \sigma_R + \sigma_I)(\omega - \sigma_R - \sigma_I)}. \quad (10)$$

Using (2) and carrying out the integration in $d\omega$ one gets

$$\begin{aligned} L_i &= \int d\omega \frac{\sum_f \langle 0 | \Theta_i^\dagger | f \rangle \langle f | \Theta_i | 0 \rangle}{(\omega - \sigma_R + \sigma_I)(\omega - \sigma_R - \sigma_I)} \delta(\omega - (E_f - E_0)) \\ &= \sum_f \langle 0 | \Theta_i^\dagger (E_f - E_0 - \sigma_R + i\sigma_I)^{-1} | f \rangle \langle f | (E_f - E_0 - \sigma_R - i\sigma_I)^{-1} \Theta_i | 0 \rangle. \end{aligned} \quad (11)$$

Then one replaces E_f by the Hamilton operator H and uses the closure property of the eigenstates of the Hamiltonian ($\sum_f |f\rangle \langle f| = 1$):

$$\begin{aligned} L_i &= \langle 0 | \Theta_i^\dagger (H - E_0 - \sigma_R + i\sigma_I)^{-1} (H - E_0 - \sigma_R - i\sigma_I)^{-1} \Theta_i | 0 \rangle \\ &\equiv \langle \tilde{\Psi}_i | \tilde{\Psi}_i \rangle \end{aligned} \quad (12)$$

with

$$|\tilde{\Psi}_i\rangle = (H - E_0 - \sigma_R - i\sigma_I)^{-1} \Theta_i | 0 \rangle. \quad (13)$$

One sees that relation (8) is indeed obtained and that $\tilde{\Psi}_i$ fulfills (6).

The standard LIT inversion method consists in the following ansatz for the response function

$$R_i(\omega', q) = \sum_{m=1}^{M_{\max}} c_m \chi_m(\omega', \alpha_j), \quad (14)$$

here the argument ω of R_i is replaced by $\omega' = \omega - \omega_{th}$, where ω_{th} is the break-up threshold of the reaction into the continuum. In case of LIT contributions attributed to bound states due to, *e.g.*, elastic transitions, one can easily subtract such contributions in order to obtain an “inelastic” LIT (see [16]). The χ_m are given functions with nonlinear parameters α_j . Normally the following basis set is taken

$$\chi_m(\omega', \alpha_j) = \omega'^{\alpha_1} \exp\left(-\frac{\alpha_2 \omega'}{m}\right). \quad (15)$$

Substituting such an expansion into the right hand side of (7) one obtains

$$L_i(\sigma_R, \sigma_I) = \sum_{m=1}^{M_{\max}} c_m \tilde{\chi}_m(\sigma_R, \sigma_I, \alpha_j), \quad (16)$$

where

$$\tilde{\chi}_m(\sigma_R, \sigma_I, \alpha_j) = \int_0^\infty d\omega' \frac{\chi_m(\omega', \alpha_j)}{(\omega' - \sigma_R)^2 + \sigma_I^2}. \quad (17)$$

For given values of α_j and M_{\max} the linear parameters c_m are determined from a best fit of $L_i(\sigma_R, \sigma_I)$ of (16) to the calculated $L_i(\sigma_R, \sigma_I)$ of (8) for a fixed σ_I and a number of σ_R points much larger than M_{\max} . In addition one should vary the various nonlinear parameter α_j over a sufficiently large range. The parameter α_1 , however, can in general be determined from the known threshold behavior of the response function. One has to increase M_{\max} up to the point that a stable inversion result is found for some range of M_{\max} values, which then can be taken as final inversion result. Note, however, that a too large value of M_{\max} might lead to an oscillatory behavior of R_i . The origin for such an unphysical behavior lies in the precision of the calculated L_i . If the precision is further increased, higher and higher M_{\max} values can in principle be used in the inversion (see also [19]).

One can repeat the whole procedure with a second σ_I value. Of course, the inversion should lead to the same R_i result as with the previous σ_I . The basis set χ_m can also be modified in order to take into account narrow structures like resonances (see section V.A). More information concerning the inversion and alternative inversion methods are found in [19].

IV. CALCULATION OF EXCLUSIVE RESPONSES WITH THE LIT METHOD

For the exclusive response function r_i one has to evaluate T-matrix elements of the type given in (4). One starts the LIT calculation using the general form of the final state wave function for the considered break-up channel [20],

$$|\Psi_f^-(E_f)\rangle = |\Phi_f(E_f)\rangle + (E_f - H - i\eta)^{-1}V|\Phi_f(E_f)\rangle, \quad (18)$$

where $|\Phi(E_f)\rangle$ is a so-called channel function (with proper antisymmetrization) given in general by the fragment bound states times their relative free motion and V is the sum of potentials acting between particles belonging to different fragments. Thus the transition matrix element $T_{0f,i}$ (additional quantum numbers are dropped) takes the following form

$$\begin{aligned} T_{0f,i} &= \langle \Psi(E_f) | \Theta_i | 0 \rangle \\ &= \langle \Phi(E_f) | \Theta_i | 0 \rangle + \langle \Phi(E_f) | V (E_f - H + i\eta)^{-1} | 0 \rangle. \end{aligned} \quad (19)$$

The first term of the right-hand-side is the so-called Born term ($T_{0f,i}^{\text{Born}}$), which can be evaluated without greater problems. The second term ($T_{0f,i}^{\text{FSI}}$) depends on the final state interaction and its evaluation is much more difficult. However, using the LIT approach, one can proceed as follows. One rewrites $T_{0f,i}^{\text{FSI}}$ in a spectral representation,

$$T_{0f,i}^{\text{FSI}} = \sum_n (E_f - E_n) F_{0f,i}(E_f, E_n) + \int_{E_{th}}^{\infty} (E_f - E' + i\eta)^{-1} F_{0f,i}(E_f, E') dE' \quad (20)$$

with

$$F_{0f,i}(E_f, E') = \sum_{\Psi_\gamma} \langle \Phi(E_f) | V | \Psi_\gamma \rangle \langle \Psi_\gamma | \Theta_i | 0 \rangle \delta(E_f - E'). \quad (21)$$

The function $F_{0f,i}$ has a similar form as an inclusive response function R_i , therefore one can apply an analogous LIT method as in the inclusive case, however left- and right-hand sides are not identical, hence two LIT equations are obtained:

$$(H - \sigma_R - i\sigma_I) |\tilde{\Psi}_i\rangle = \Theta_i | 0 \rangle, \quad (H - \sigma_R - i\sigma_I) |\tilde{\Psi}_V\rangle = V |\Phi(E_f)\rangle. \quad (22)$$

The first one is essentially the same as (6). The second equation has a different right-hand side, but with the important feature to vanish asymptotically for a nuclear potential V . Therefore the equation can again be solved with a bound-state technique. In case of an additional Coulomb interaction, one may use Coulomb wave functions instead of the free motion $|\Phi_f\rangle$ if only two of the fragments carry charge.

Having calculated $\tilde{\Psi}_i$ and $\tilde{\Psi}_V$ one evaluates the overlap $\langle \tilde{\Psi}_V | \tilde{\Psi}_i \rangle$, which is identical to the LIT of the function $F_{0f,i}$, and hence $F_{0f,i}$ is obtained by the inversion of the LIT. The FSI part of the T-matrix element is then given by

$$T_{0f,i}^{\text{FSI}}(E_f) = -i\pi F_{0f,i}(E_f, E_f) + \mathcal{P} \int_{E_{th}^-}^{\infty} (E_f - E')^{-1} F_{0f,i}(E_f, E') dE' \quad (23)$$

and the sum of $T_{0f,i}^{\text{FSI}}$ and the simpler Born term $T_{0f,i}^{\text{Born}}$ leads to the total result for the transition matrix element.

As shown in [16] the LIT formalism for exclusive reactions can be reformulated such that only a solution for $\tilde{\Psi}_i$ is requested, while $\tilde{\Psi}_V$ is not needed. Both possibilities have been used in [21], where the $d(e, e'p)n$ reaction has been calculated as a test case for the exclusive LIT formalism.

V. APPLICATION OF THE LIT METHOD

As we have shown in the previous sections the main point of the LIT approach consists in the fact that a scattering state problem is reduced to a bound-state-like problem. In other words the calculation of continuum wave functions is not required, instead one has to solve equations which can be solved with bound-state techniques. For $A > 2$ the calculation of continuum wave functions is difficult or today even impossible, thus, with the LIT method, one can extend the range of calculations to considerably larger A . In fact one may conclude the following: if one is able to carry out a bound-state calculation for a given particle system then the LIT approach opens up the possibility to perform calculations for continuum reactions with this particle system. In principle one is not restricted to use a specific bound-state technique, but in most LIT calculations an expansion of ground state $|0\rangle$ and LIT function $|\tilde{\Psi}\rangle$ in hyperspherical harmonics (HH) is employed. Information concerning such expansions is given in [16], here we only want to mention that the realistic LIT applications for $A=3$ have been performed with the CHH technique [22], whereas the realistic (semirealistic) applications for $A=4$ ($A > 4$) have been carried out with the EIHH approach [23].

For the solution of the LIT equation (6) the Lanczos method is used in most cases [24]. In this context it should be pointed out that the LIT method is different from an approach where a so-called Lanczos response R_{Lanc} is introduced, which is essentially a LIT with small

σ_I , which, however, is directly interpreted – without any inversion – as a response function (for more details see [16]).

A. Simple example: deuteron photodisintegration

In order to illustrate how the method works we first apply the LIT approach to a very simple physical problem, namely to the total deuteron photoabsorption cross section in unretarded dipole approximation. In this case the cross section is given by

$$\sigma_\gamma^d(\omega) = 4\pi^2\alpha\omega R_\gamma^d(\omega), \quad (24)$$

where α is the fine structure constant, ω is the energy of the photon absorbed by the deuteron, and $R_\gamma^d(\omega)$ denotes the response function defined as

$$R_\gamma^d(\omega) = \sum_f |\langle f | \Theta | 0 \rangle|^2 \delta(\omega - E_{np} - E_d). \quad (25)$$

Here E_d and $|0\rangle$ are the deuteron bound state energy and wave function, while E_{np} and $|f\rangle$ denote relative kinetic energy and wave function of the outgoing np pair for a given two-nucleon Hamiltonian H :

$$(H + E_d)|0\rangle = 0, \quad (H - E_{np})|f\rangle = 0. \quad (26)$$

The transition operator Θ is defined by

$$\Theta = \sum_{i=1}^2 z_i \tau_i^3, \quad (27)$$

where z_i and τ_i^3 are the third components of position and isospin coordinates of the i -th nucleon. The LIT of R_γ^d is given by

$$L_\gamma^d(\sigma_R, \sigma_I) = \sum_{k=1}^3 \langle \tilde{\Psi}_k | \tilde{\Psi}_k \rangle = \int R_\gamma^d(\omega) \mathcal{L}(\omega, \sigma_R, \sigma_I) d\omega, \quad (28)$$

where $k = 1, 2, 3$ correspond to different partial waves of the final state, namely 3P_0 , 3P_1 , and ${}^3P_2 - {}^3F_2$.

First we consider deuteron photodisintegration with a realistic NN interaction. In the already mentioned review article of the LIT method [16], such a case has been investigated using the AV14 NN potential [25]. The L_γ^d result is shown in Fig. 1, while the corresponding

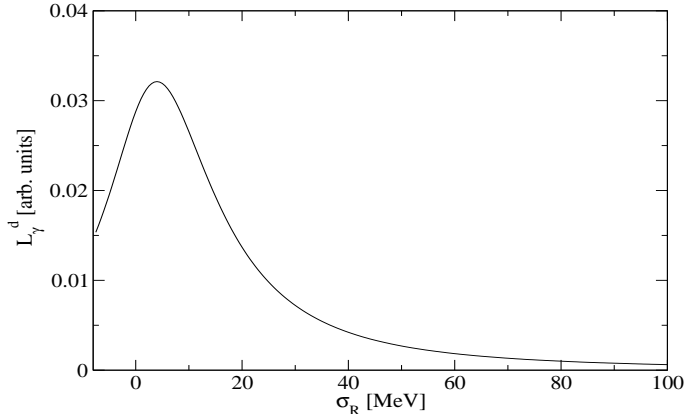


FIG. 1: LIT L_γ^d with $\sigma_I=10$ MeV.

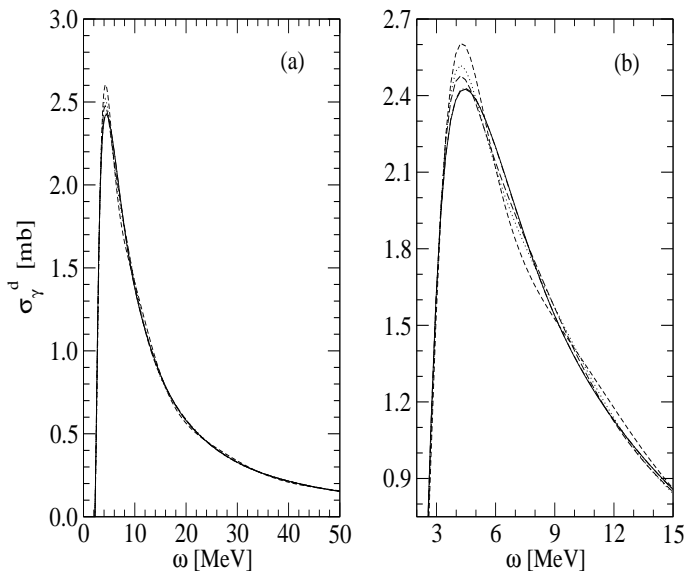


FIG. 2: σ_γ^d from inversion of L_γ^d of Fig. 1, up to 50 MeV (a) and in peak region (b), with various M_{\max} values: 10 (short dashed), 15 (dotted), 20 (long dashed), 25 (solid), 26 (dash-dotted).

inversion results are illustrated in Fig. 2. For the inversion one observes a nice stability range of the results for all the shown M_{\max} values in the whole considered energy range, except for the peak region, where the inversion becomes stable only for higher M_{\max} . One notes that the M_{\max} values 25 and 26 lead essentially to identical results.

In Fig. 3 the final inversion result ($M_{\max}=25$) is compared with the corresponding cross section of a conventional calculation with explicit np continuum wave functions [16]. One

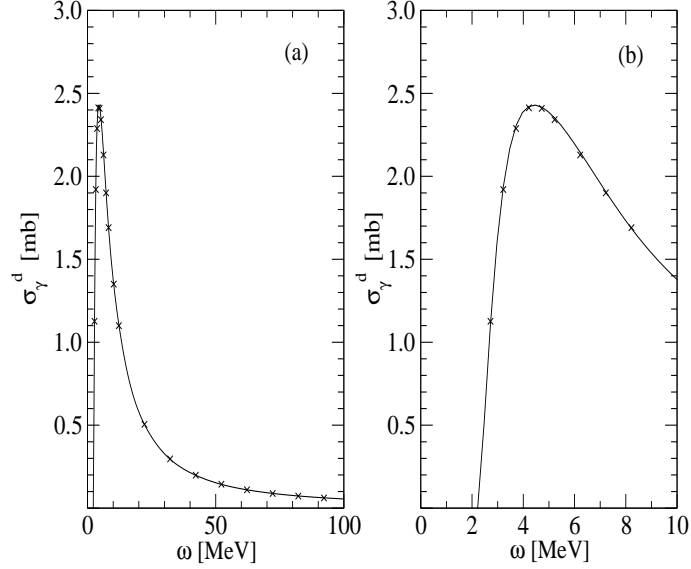


FIG. 3: Total deuteron photoabsorption cross section up to 50 MeV (a) and in peak region (b): LIT result (solid) and from calculation with explicit np continuum wave functions (crosses).

finds an excellent agreement between the two calculations showing that one can reach high-precision results with the LIT method.

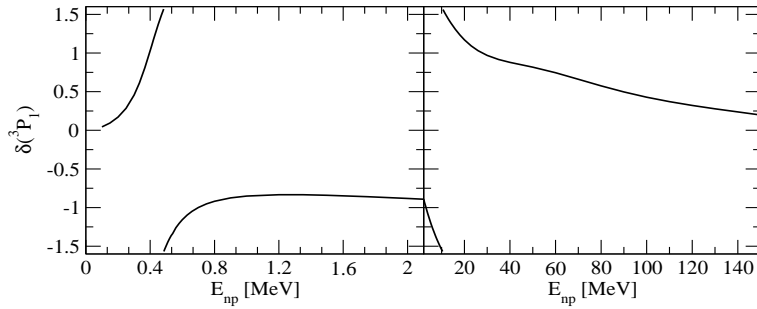


FIG. 4: Phase shift 3P_1 of fictitious np system at low (left) and higher (right) energies.

Further LIT calculations for the deuteron total photoabsorption cross sections have already been discussed in [26, 27]. For the aim of the present discussion, *i.e.* the way of working of the LIT method, [27] is particularly interesting. It is a case study for a fictitious np system with a low-lying and narrow resonance in the 3P_1 nucleon-nucleon partial wave (obtained by an additional attractive term, for details see [27]). The results of a conventional calculation with the fictitious np system for the 3P_1 phase shifts and the “deuteron

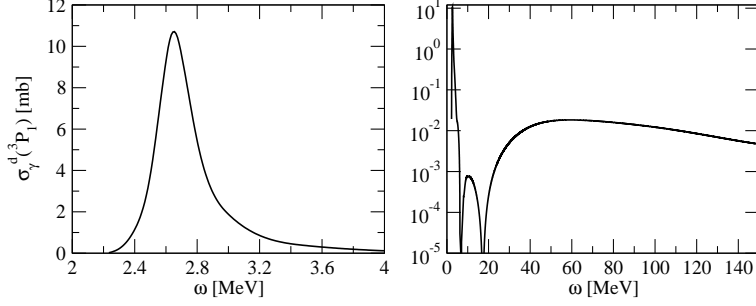


FIG. 5: As Fig. 4 but for photodisintegration cross section.

photoabsorption cross section” to the 3P_1 final state are shown in Figs. 4 and 5, respectively. The 3P_1 phase shifts exhibit two resonances, at $E_{np} = 0.48$ MeV and at about $E_{np} = 10.5$ MeV. The low-energy resonance leads to the dominant structure of the photoabsorption cross section, a pronounced peak at a photon energy of 2.65 MeV with a width Γ of 270 keV, while the second resonance only shows up as a rather tiny peak, which is more than four orders of magnitude smaller than the first peak.

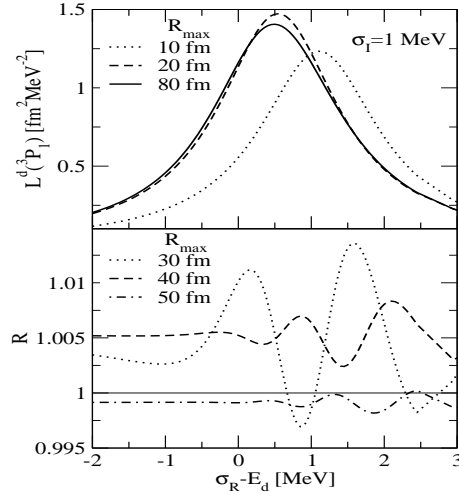


FIG. 6: LIT $L_\gamma^d(^3P_1)$ of fictitious np system in first resonance region with $\sigma_I = 1$ MeV and various values of R_{\max} (top) and ratio $R=L_\gamma^d(R_{\max})/L_\gamma^d(R_{\max} = 80 \text{ fm})$ (bottom).

For the LIT calculation of the photoabsorption cross section of the fictitious np system the inversion basis set χ_m (15) is modified to account for the resonant structure, to this end

the functions χ_m are relabeled: $\chi_m \rightarrow \chi_{m+1}$. In addition a new χ_1 is defined,

$$\chi_1(E_{np}, \alpha_i) = \frac{1}{(E_{np} - E_{\text{res}})^2 + (\frac{\Gamma}{2})^2} \left(\frac{1}{1 + \exp(-1)} - \frac{1}{1 + \exp((E_{np} - \alpha_3)/\alpha_3)} \right), \quad (29)$$

where $E_{\text{res}} \equiv \alpha_4$, $\Gamma \equiv \alpha_5$ and α_3 are additional nonlinear parameters.

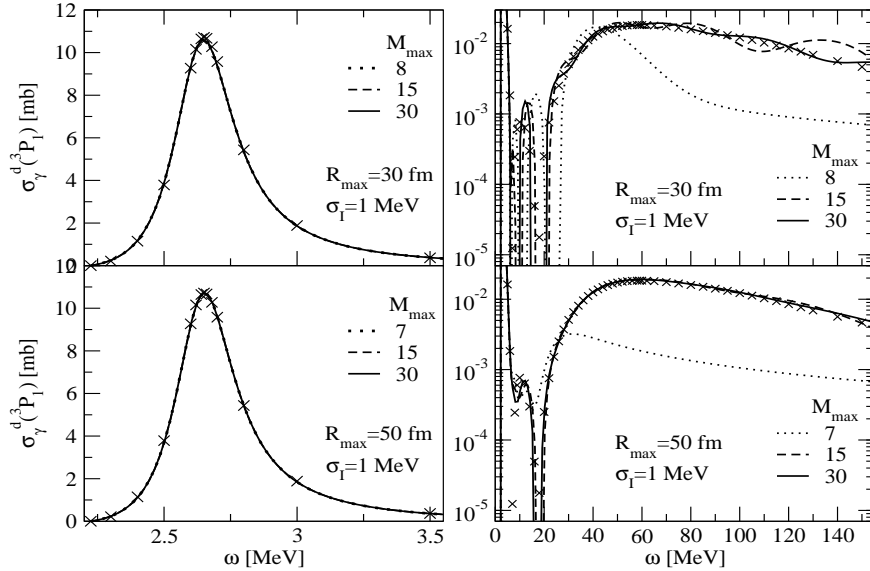


FIG. 7: $\sigma_\gamma^d(^3P_1)$ of fictitious np system from inversion of $L_\gamma^d(^3P_1, \sigma_I = 1 \text{ MeV}, R_{\text{max}})$ with various M_{max} values and $R_{\text{max}} = 30 \text{ fm}$ (top) and 50 fm (bottom) in first resonance region (left) and beyond (right); also shown results of a conventional calculation with explicit np continuum wave functions (crosses).

The reason for such a LIT case study with a resonance lies in the results of a previous LIT calculation for the (e, e') longitudinal and transverse form factors of ^4He [28], where a resonance in the Coulomb monopole transition was obtained, but its width could not be determined. In the case study it is shown that for a proper resolution of a resonant structure it is very important to take into account the LIT function $\tilde{\Psi}$ up to rather large distances [27]. This has been checked (i) by solving (6) imposing at a two-nucleon distance $r = R_{\text{max}}$ an asymptotic boundary condition which leads to a strong fall-off of $\tilde{\Psi}(^3P_1)$ and (ii) by calculating the norm $\langle \tilde{\Psi}(^3P_1) | \tilde{\Psi}(^3P_1) \rangle$ only in the range from $r = 0$ to $r = R_{\text{max}}$. In Fig. 6 we show the results for such a calculation choosing $\sigma_I = 1 \text{ MeV}$. One notes that for a rather precise result, with errors below about 1%, one has to take $R_{\text{max}} \geq 30 \text{ fm}$. A further increase of R_{max} to 50 fm leads to a reduction of the relative error by about a factor ten. In

Fig. 7 the inversions results with $R_{\max} = 30$ and 50 fm are depicted in comparison to the result of the direct calculation. One observes that for both R_{\max} values the resonance cross section is described with high accuracy. Differences between the two cases become evident in the region of the second maximum and at higher energy. In fact with $R_{\max} = 30$ fm one finds only a reasonably good description, while a considerable improvement is obtained with $R_{\max} = 50$ fm.

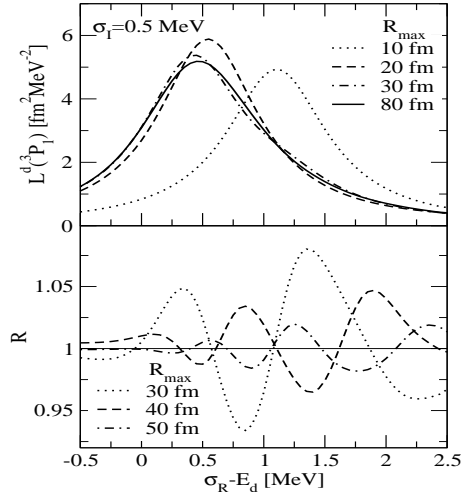


FIG. 8: As Fig. 6 but with $\sigma_I = 0.5$ MeV

As next point we consider the reduction of σ_I from 1 MeV to 0.5 MeV. As shown in Fig. 8 one finds an enhancement of the relative error of L^d_γ by at least a factor of five in comparison to the corresponding R_{\max} values of Fig. 6. The enhancement is easily understood by investigating the asymptotic solution of (6); in the here considered deuteron case it is described by the exponential fall-off $\exp(-r(M\sigma_I)^{1/2}/\hbar)$, where M is the nucleon mass. It is evident that a smaller σ_I leads to a longer range LIT function $\tilde{\Psi}$. As discussed in [27], for $\sigma_I = 0.1$ MeV even $R_{\max} = 300$ fm is not completely sufficient, since only the resonance itself is resolved, but not the cross section at higher energies.

The discussion above seems to infer that it is better to choose a rather large value for σ_I . On the other hand it should also be clear that the width of the resonance Γ and the value of σ_I are correlated. If σ_I is too large the resonance cannot be resolved. In the case study it has been found that $\sigma_I = 2$ MeV, about seven times larger than the width Γ , is still sufficient for a resolution of the resonance. However, in a general case the resonance width is not known beforehand and the question arises what should be the proper value for

σ_I in such a case. As pointed out in [27] one has to proceed as follows. One performs a LIT calculation with a given σ_I and compares the result to a LIT with a δ -peak in the response function or cross section. For example, in the here discussed deuteron case one sets

$$R_\gamma^{\text{peak}}(E_{np}) = R^{\text{peak}} \delta(E_{np} - E^{\text{peak}}).$$

The resulting δ -LIT is then given by the Lorentzian function

$$L_\delta^d(E^{\text{peak}}, \sigma_R, \sigma_I) = R^{\text{peak}} \mathcal{L}(E^{\text{peak}}, \sigma_R, \sigma_I),$$

where R^{peak} is chosen such that the peak heights of L_δ^d and L_γ^d are equal.

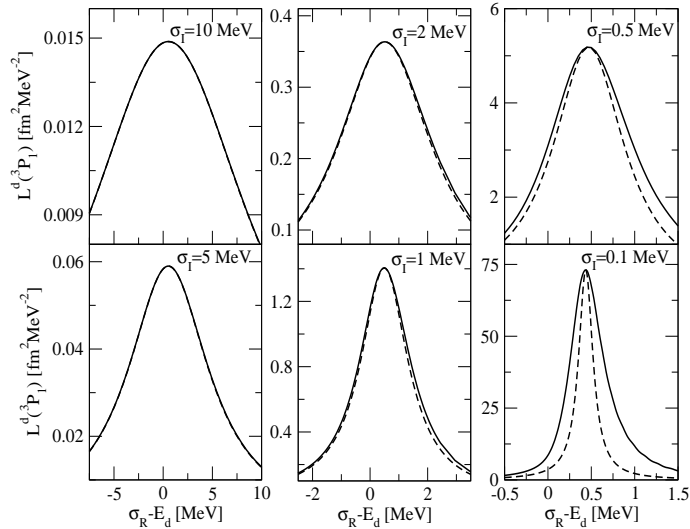


FIG. 9: LIT $L^d(^3P_1)$ (full curves) and L_δ^d (dashed curves) of fictitious np system in first resonance region with various σ_I values and $R_{\text{max}} = 80$ fm, except for $\sigma_I = 0.1$ MeV where $R_{\text{max}}=300$ fm.

In order to obtain a reliable inversion the actual LIT L_γ^d should have a larger width than the δ -LIT L_δ^d . If, on the contrary, they lead to essentially identical results, one has to reduce σ_I up to the point that the actual LIT is sufficiently different from the corresponding δ -LIT. In Fig. 9 we show such results for the deuteron case study. For $\sigma_I=5$ and 10 MeV there are practically no differences between LIT and δ -LIT, while for $\sigma_I \leq 2$ MeV differences become visible. As a matter of fact $\sigma_I=2$ MeV is sufficient for a reliable inversion and thus one may conclude that in a general case one has to use a σ_I such that differences between LIT and δ -LIT have at least the same size as in the $\sigma_I=2$ MeV case of Fig. 9.

In Fig. 10 we show the final inversion results from [27] with $R_{\max} = 80$ fm. One sees that the E1 resonance is precisely described with the LIT method for $\sigma_I = 0.5$ and 2 MeV, while the peak is somewhat underestimated with $\sigma_I = 5$ MeV. In the resonance region, with the two lower σ_I values, essentially the same results are obtained as for the cases of Fig. 7 with $\sigma_I = 1$ MeV and $R_{\max} = 30$ and 50 fm. From the comparison one further notes that the case $\sigma_I = 2$ MeV and $R_{\max} = 80$ fm leads to even more precise results in the second resonance region, and beyond, than shown in Fig. 7 for $R_{\max} = 50$ fm.

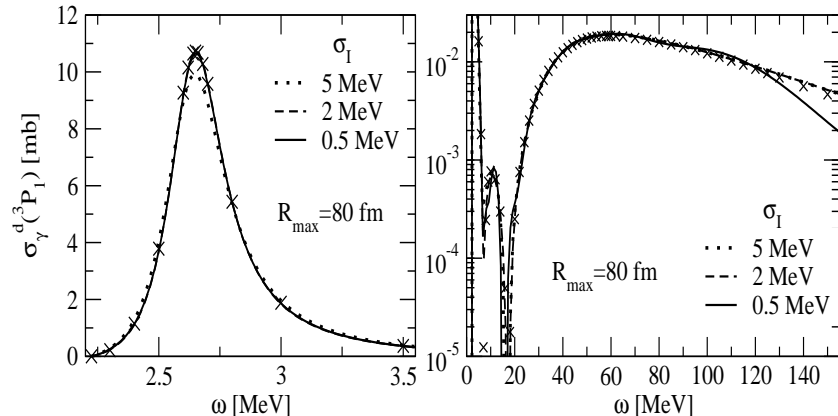


FIG. 10: As Fig. 7 but with $R_{\max} = 80$ fm and $\sigma_I = 5, 2,$ and 0.5 MeV.

B. Reactions with $A \geq 3$

Now we turn to realistic applications of the LIT method and consider first the ${}^4\text{He}$ total photoabsorption cross section. In fact this is one of the very first LIT applications [7], however, initially only performed with semirealistic NN forces. In [7] it has been found that the calculated cross section shows a considerably more pronounced giant dipole resonance than the most recent experimental data of that time. Such a difference between experiment and an *ab initio* calculation has led to a renewed experimental interest in the ${}^4\text{He}$ photoabsorption cross section. In fact in the meantime three additional experiments have been carried out [29, 30, 31]. Finally, in [5] the first calculation with realistic NN and 3N forces has also been published. In Fig. 11 we show the theoretical results of [5] together with the experimental data. One notes that the 3N force leads to a considerable reduction of the peak cross section. One further sees that there is a very good agreement between theory and the data

of [31] and also quite a good agreement with the data of [29], while the cross section of [30] shows a completely different behavior. Also shown in the figure are data from experiments performed about 20 years ago.

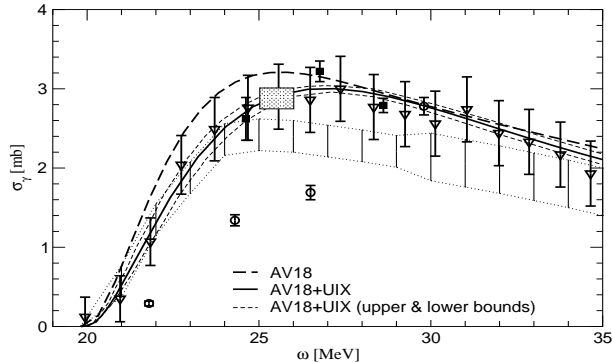


FIG. 11: Total ${}^4\text{He}$ photoabsorption cross section: LIT calculation with AV18 NN potential only [32], and with additional UIX 3N force [33]; experimental data: squares [29], circles [30], triangles [31], area between dotted lines [34, 35], and dotted box [36].

It should be mentioned that today two other LIT calculations for the ${}^4\text{He}$ total photoabsorption cross section are available [37, 38], where different realistic nuclear forces have been used. Essentially, they confirm the results of [5].

In Fig. 12 LIT results for the ${}^6\text{Li}$ and ${}^6\text{He}$ total photoabsorption cross sections calculated with semirealistic NN forces are shown [8]. For ${}^6\text{Li}$ one finds a single and rather broad cross section peak. On the contrary for ${}^6\text{He}$ a very interesting cross section with a double peak becomes apparent in the calculation. This microscopic result can be interpreted as follows. In a cluster picture, with an α core and a di-neutron, the low-energy peak is due to the relative motion of di-neutron and α core. The second peak, however, cannot be obtained in a cluster model, but is explained by the classical E1 giant resonance picture with a collective response of all nucleons (relative motion of protons and neutrons). For ${}^6\text{Li}$, in a cluster model described by an α core plus a deuteron, a similar low-energy peak is missing, because the deuteron knock-out corresponds to an isoscalar transition, which cannot be induced by the isovector dipole operator (27). On the other hand a transition to the antibound ${}^1S_0(np)$ plus α core is possible. The nucleus ${}^6\text{Li}$ exhibits a considerably larger width of the giant

dipole peak than ${}^6\text{He}$. In fact in the former a break-up into two three-body nuclei is possible (${}^3\text{H}-{}^3\text{He}$), while a similar break-up of ${}^6\text{He}$ is not induced by the dipole operator, since the ${}^3\text{H}-{}^3\text{H}$ pair has no dipole moment. The experimental ${}^6\text{He}$ and ${}^6\text{Li}$ photoabsorption cross sections are not yet well settled (see [8]) and therefore not shown here.

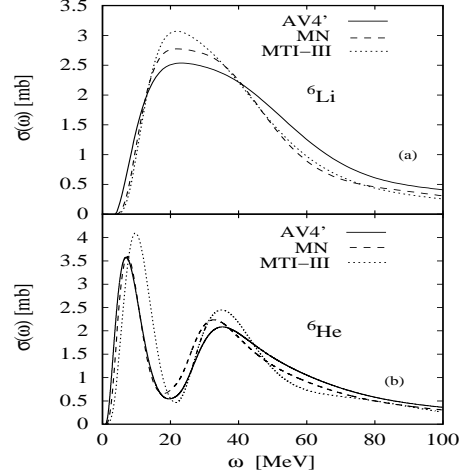


FIG. 12: ${}^6\text{Li}$ and ${}^6\text{He}$ total photoabsorption cross sections with various semirealistic NN potential models: AV4' [39], MN [40], and MTI-III [41].

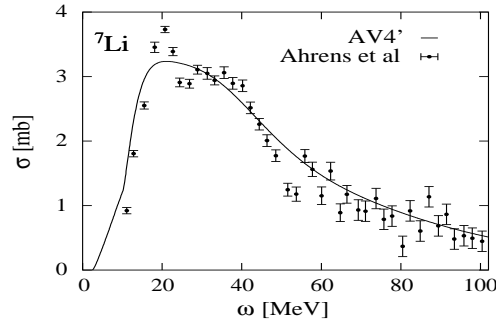


FIG. 13: ${}^7\text{Li}$ total photoabsorption cross section with semirealistic NN potential model AV4', experimental data from [42].

In Fig. 13 we depict the LIT calculation for the ${}^7\text{Li}$ total photoabsorption cross section [9], in comparison to experimental data [42]. It is worthwhile to mention that the experimental

cross section has not been determined by summing up the various channel cross sections, but in a single experiment by the “diminution of photon flux” method. Like ${}^6\text{Li}$ also ${}^7\text{Li}$ has a giant dipole resonance peak with a rather large width. The comparison of experimental and theoretical results shows quite a good agreement, though only a semirealistic NN force has been used in the LIT calculation. Of course, it would be very interesting to have even more precise data and also a calculation with realistic nuclear forces.

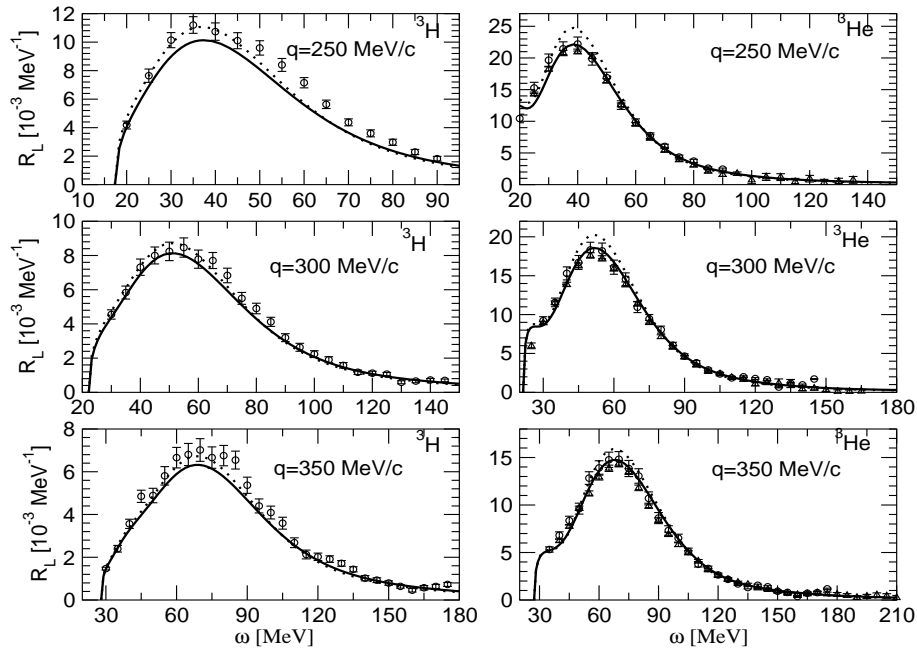


FIG. 14: $R_L(\omega, q)$ of ${}^3\text{H}$ (left) and ${}^3\text{He}$ (right) at various q : AV18 NN potential (dotted), AV18 NN + UIX 3N potential (solid); experimental data: triangles [44], and circles [45].

Now we turn to the inclusive electron scattering response functions. For ${}^3\text{H}$ and ${}^3\text{He}$ LIT calculations for the longitudinal response function $R_L(\omega, q)$ have been carried out with realistic nuclear forces for momentum transfers below [43], and above $q=500$ MeV/c [11]. Relativistic corrections for the transition operator O_L have been taken into account and the frame dependence of the essentially nonrelativistic calculation has been studied. In Fig. 14 R_L is shown for various lower q values [43]. One notes that the 3N force reduces the quasielastic peak height somewhat. The 3N force effect, however, does not lead to a consistent picture in comparison with experiment. In fact one finds an improvement for ${}^3\text{He}$ and a deterioration for ${}^3\text{H}$.

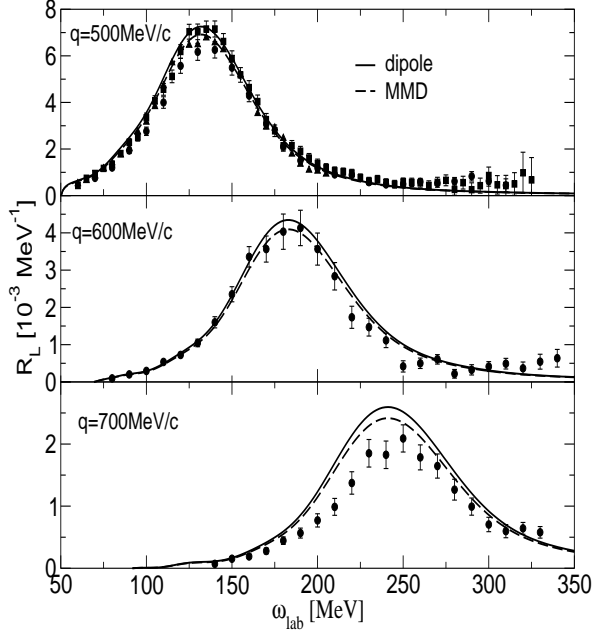


FIG. 15: $R_L(\omega, q)$ of ${}^3\text{He}$ at various q , calculation with AV18 NN + UIX 3N potentials and two nucleon form factors fits: dipole (solid) and MMD from [47] (dashed); experimental data: squares [44], triangles [45], and circles [46].

In [11] it has been found that relativistic effects due to the kinetic energy can be largely reduced if R_L is first calculated in a specific reference frame, where the target nucleus moves with $-\mathbf{A}\mathbf{q}/2$, and then transformed to the lab system. Different from a direct calculation in the lab system, one finds a correct result for the experimentally established quasielastic peak position [11], as shown in Fig. 15. At $q=500$ and 600 MeV/ c also for the peak height a good agreement with experimental data is obtained, whereas the theoretical R_L overestimates the experimental one at $q=700$ MeV/ c (at even higher q experimental data are not available). As Fig. 15 shows also the choice of the nucleon form factor fit has a non-negligible impact on the result, but cannot explain the discrepancy with the data at $q = 700$ MeV/ c .

Recently we also calculated the transverse response function $R_T(\omega, q)$ with realistic nuclear forces ($q \leq 500$ MeV/ c) [12]. Besides the usual one-body operators also π and ρ exchange currents (EC), consistent with the NN potential model, were taken into account. In addition also the effect of the so-called Siegert operator has been studied. In Fig. 16 the theoretical results are shown together with experimental data. In the quasielastic region EC lead to some increase of the peak height (see left panels of Fig. 16), but the EC effect

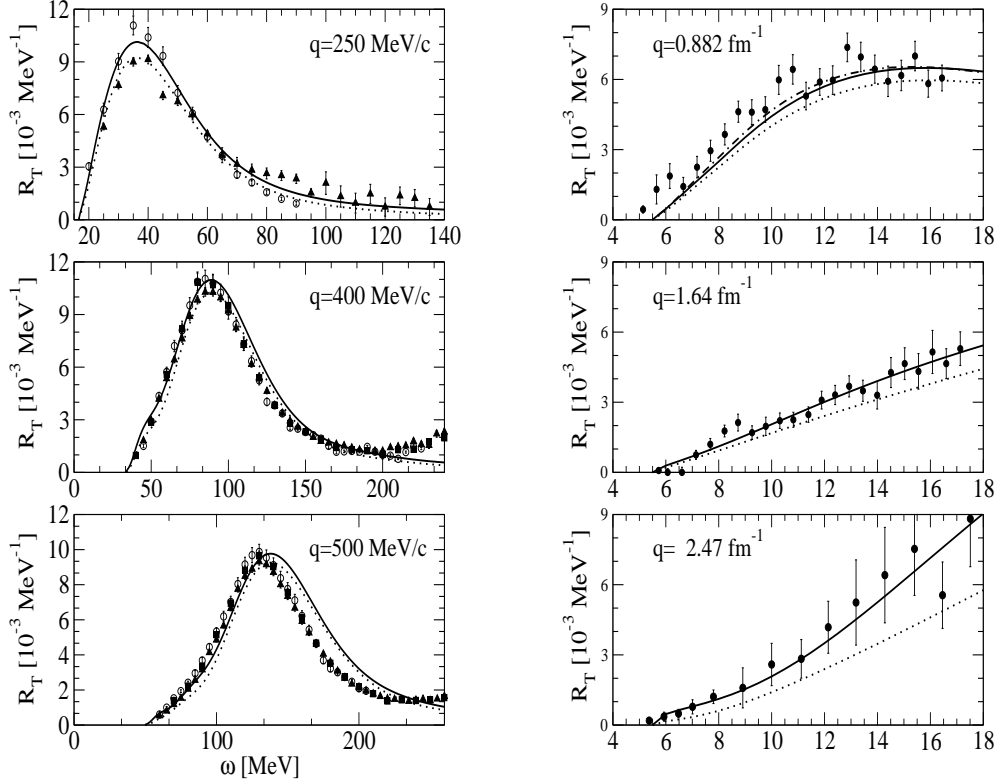


FIG. 16: $R_T(\omega, q)$ in quasielastic (left) and threshold region (right), theoretical results with BonnRA NN potential [48], and TM' 3N forces [49], and following current operators: one-body (dotted) and one-body + π -EC + ρ -EC + additional EC via Siegert operator (solid). Experimental data: left panels, triangles [44], circles [45], and squares [46]; and right panels, circles [50].

is much larger close to threshold (see right panels of Fig. 16) and is important for a good agreement of theory and experiment. For $q=500$ MeV/c one finds different peak positions in theory and experiment, presumably due to the fact that R_T is calculated directly in the lab frame (see discussion above). The frame dependence of R_T is presently under investigation.

Presently we are extending our realistic calculation to the (e, e') response functions of ${}^4\text{He}$ and results for R_L will be published soon.

Summarizing one may conclude that the LIT method is very powerful and allows a considerable extension of the range of microscopic *ab initio* calculations.

-
- [1] V. D. Efros, W. Leidemann, and G. Orlandini, *Phys. Lett.* **B338**, 130 (1994).
- [2] V. D. Efros, *Yad. Fiz.* **41**, 1498 (1985) [*Sov. J. Nucl. Phys.* **41**, 949 (1985)].
- [3] V. D. Efros, W. Leidemann, and G. Orlandini, *Few-Body Syst.* **14**, 151 (1993).
- [4] V. D. Efros, W. Leidemann, G. Orlandini, and E. L. Tomusiak, *Phys. Lett.* **B484**, 223 (2000).
- [5] D. Gazit *et al.*, *Phys. Rev. Lett.* **96**, 112301 (2006).
- [6] D. Gazit and N. Barnea, *Phys. Rev. Lett.* **98**, 192501 (2007).
- [7] V. D. Efros, W. Leidemann, and G. Orlandini, *Phys. Rev. Lett.* **78**, 4015 (1997); N. Barnea, V. D. Efros, W. Leidemann, and G. Orlandini, *Phys. Rev.* **C63**, 057002 (2001).
- [8] S. Bacca *et al.*, *Phys. Rev. Lett.* **89**, 052502 (2002); S. Bacca, N. Barnea, W. Leidemann, and G. Orlandini, *Phys. Rev.* **C69**, 057001 (2004).
- [9] S. Bacca *et al.*, *Phys. Lett.* **B603**, 159 (2004).
- [10] V. D. Efros, W. Leidemann, and G. Orlandini, *Phys. Rev. Lett.* **78**, 432 (1997).
- [11] V. D. Efros, W. Leidemann, G. Orlandini, and E. L. Tomusiak, *Phys. Rev.* **C72**, 011002(R) (2005).
- [12] S. Della Monaca *et al.*, *Phys. Rev.* **C77**, 044007 (2008).
- [13] S. Quaglioni *et al.*, *Phys. Rev.* **C69**, 044002 (2004).
- [14] S. Quaglioni, V. D. Efros, W. Leidemann, and G. Orlandini, *Phys. Rev.* **C72**, 064002 (2005).
- [15] D. Andreasi *et al.*, *Eur. Phys. J.* **A27**, 47 (2006).
- [16] V. D. Efros, W. Leidemann, G. Orlandini, and N. Barnea, *J. Phys.* **G34**, R459 (2007).
- [17] J. D. Walecka, *Theoretical Nuclear and Subnuclear Physics* (World Scientific, Singapore, 2004).
- [18] H. Arenhövel, W. Leidemann, and E. L. Tomusiak, *Eur. Phys. J.* **A23**, 147 (2005).
- [19] D. Andreasi, W. Leidemann, Ch. Reiss, and M. Schwamb, *Eur. Phys. J.* **A24**, 361 (2005).
- [20] M. L. Goldberger and K. W. Watson, *Collision Theory* (Wiley, New York, 1964).
- [21] A. La Piana and W. Leidemann, *Nucl. Phys.* **A677**, 423 (2000).
- [22] Yu. I. Fenin and V. D. Efros, *Yad. Fiz.* **15**, 887 (1972) [*Sov. J. Nucl. Phys.* **15**, 497 (1972)]; W. Leidemann, V. D. Efros, G. Orlandini, and E. L. Tomusiak, *Fizika* **B8**, 135 (1999).
- [23] N. Barnea, W. Leidemann, and G. Orlandini, *Phys. Rev.* **C61**, 054001 (2000); N. Barnea, W. Leidemann, and G. Orlandini, *Nucl. Phys.* **A693**, 565 (2001).
- [24] M. Marchisio, N. Barnea, W. Leidemann, and G. Orlandini, *Few-Body Syst.* **33**, 259 (2003).

- [25] R. B. Wiringa, R. A. Smith, and T. L. Ainsworth, *Phys. Rev.* **C29**, 1207 (1984).
- [26] N. Barnea, W. Leidemann, and G. Orlandini, *Phys. Rev.* **C74**, 034003 (2006).
- [27] W. Leidemann, *Few-Body Syst.* in print, arXiv:0803.1770.
- [28] S. Bacca *et al.* *Phys. Rev.* **C76**, 014003 (2007).
- [29] B. Nilsson *et al.*, *Phys. Lett.* **B626**, 65 (2005).
- [30] T. Shima *et al.*, *Phys. Rev.* **C72**, 044004 (2005).
- [31] S. Nakayama *et al.*, *Phys. Rev.* **C76**, 021305(R) (2007).
- [32] R. B. Wiringa, V. G. J. Stoks, and R. Schiavilla, *Phys. Rev.* **C51**, 38 (1995).
- [33] B. S. Pudliner *et al.*, *Phys. Rev.* **C56**, 1720 (1997).
- [34] B. L. Berman, D. D. Faul, P. Meyer, and D. L. Olson, *Phys. Rev.* **C22**, 2273 (1980).
- [35] G. Feldman *et al.*, *Phys. Rev.* **C42**, R1167 (1990).
- [36] D. P. Wells *et al.*, *Phys. Rev.* **C46**, 449 (1992).
- [37] S. Bacca, *Phys. Rev.* **C75**, 044001 (2007).
- [38] S. Quaglioni and P. Navrátil, *Phys. Lett.* **B652**, 370 (2007).
- [39] R. B. Wiringa and S. C. Pieper, *Phys. Rev. Lett.* **89**, 182501 (2002).
- [40] D. R. Thomson, M. LeMere, and Y. C. Tang, *Nucl. Phys.* **A286**, 53 (1977); I. Reichstein and Y. C. Tang, *ibid.* **A158**, 529 (1970).
- [41] R. A. Malfliet and J. Tjon, *Nucl. Phys.* **A127**, 161 (1969).
- [42] J. Ahrens *et al.*, *Nucl. Phys.* **A251**, 479 (1975).
- [43] V. D. Efros, W. Leidemann, G. Orlandini, and E. L. Tomusiak, *Phys. Rev.* **C69**, 044001 (2004).
- [44] C. Marchand *et al.*, *Phys. Lett.* **B153**, 29 (1985).
- [45] K. Dow *et al.*, *Phys. Rev. Lett.* **61**, 1706 (1988).
- [46] J. Carlson, J. Jourdan, R. Schiavilla, and I. Sick, *Phys. Rev.* **C65**, 024002 (2002).
- [47] P. Mergell, U.-G. Meissner, and D. Drechsel, *Nucl. Phys.* **A596**, 367 (1996).
- [48] R. Machleidt, *Adv. Nucl. Phys.* **19**, 189 (1989).
- [49] S. A. Coon *et al.*, *Nucl. Phys.* **A317**, 242 (1979).
- [50] G. A. Retzlaff *et al.*, *Phys. Rev.* **C49**, 1263 (1994).